# Electroweak penguin decays at LHC*b*

($B_d \to K^{*0}\mu^+\mu^-$, $B_d \to K^{*0}\gamma$ and $B_s \to \phi\gamma$)

DPF 2011, Brown University

T. Blake on behalf of LHC*b*

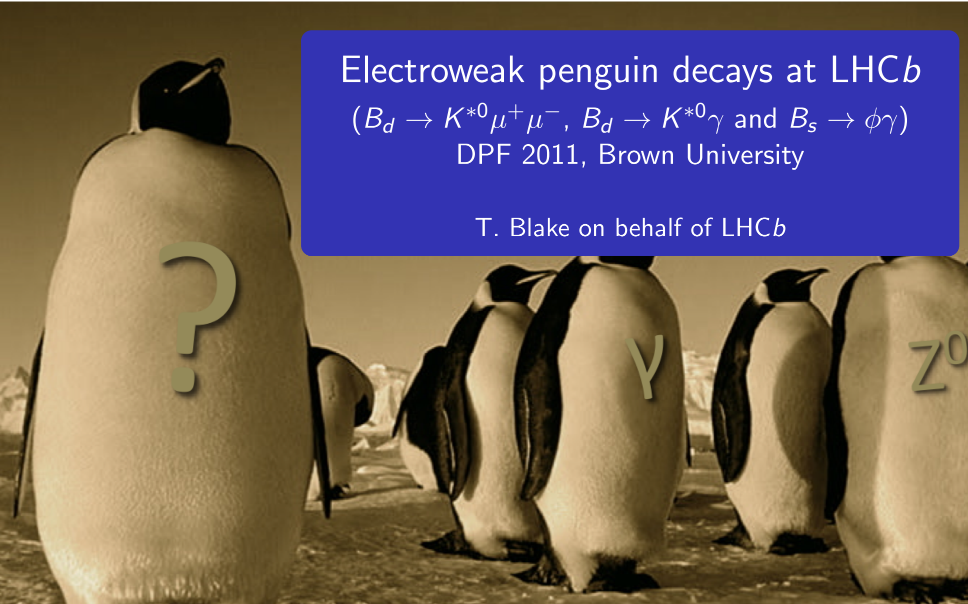

# Outline

1. Introduction
   - Probing new physics with rare decays
   - The LHCb detector
2. Results

# Why study "rare" decays of $B_s$ and $B_d$ mesons?

- FCNC processes, mediated by electroweak box and penguin diagrams in SM, i.e. only possible through loops.
- New Physics enters at same (i.e. loop) order and can give rise to comparably large deviations from SM predictions in:
  - Branching fractions.
  - Angular distributions.
  - CP and Isospin asymmetries.

$\rightarrow$ Sensitivity to larger mass scales than those directly accessible at the LHC.

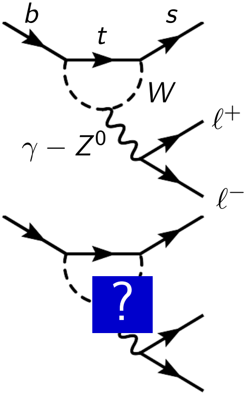

# Sensitivity to NP through rare decays

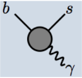


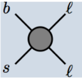


| Operator $\mathcal{O}_i$ | |
|---|---|
| $\mathcal{O}_7 \sim m_b(\bar{s}_L \sigma_{\mu\nu} b_R)F_{\mu\nu}$ | $b \to s\gamma$ & $b \to s\ell\ell$ |
| $\mathcal{O}_9 \sim (\bar{s}b)_{V-A}(\bar{\ell}\ell)_V$ | $b \to s\ell\ell$ |
| $\mathcal{O}_{10} \sim (\bar{s}b)_{V-A}(\bar{\ell}\ell)_A$ | $b \to s\ell\ell$ |
| $\mathcal{O}_{S,P} \sim (\bar{s}b)_{S+P}(\bar{\ell}\ell)_{S,P}$ | $B_s \to \mu^+\mu^-$ & $b \to s\ell\ell$ |

In the SM:

- $\mathcal{C}_{S,P} \propto m_\ell m_b / m_W^2 \sim 0$.
- Helicity flipped operators $(\mathcal{C}'_i \mathcal{O}'_i)$ suppressed by $m_s/m_b$.

# The LHCb detector

Forward arm spectrometer covering $2 < \eta < 5$.

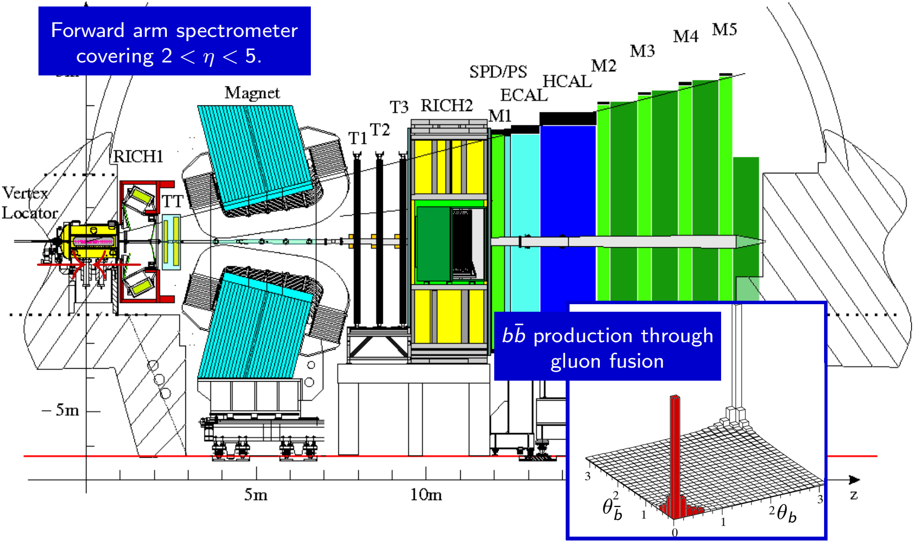


$b\bar{b}$ production through gluon fusion

# Needle in a haystack?

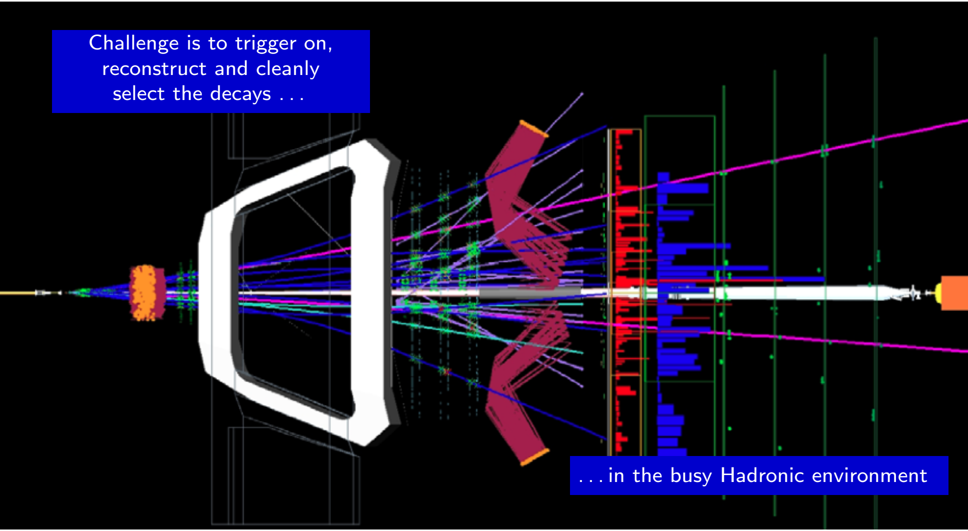

# Data taking

- Excellent performance from LHC in 2010-2011.
- Results presented for $B_d \to K^{*0}\mu^+\mu^-$ are based on $309\,\mathrm{pb}^{-1}$ collected in 3 months in 2011.
- Results presented for $B_d \to K^{*0}\gamma$ and $B_s \to \phi\gamma$ are based on $88\,\mathrm{pb}^{-1}$ collected in 2010 + 2011.
- Instantaneous luminosities of $\sim 3 \times 10^{32}\,\mathrm{cm}^{-2}\mathrm{s}^{-1}$. We are already at design luminosity in LHC*b*.

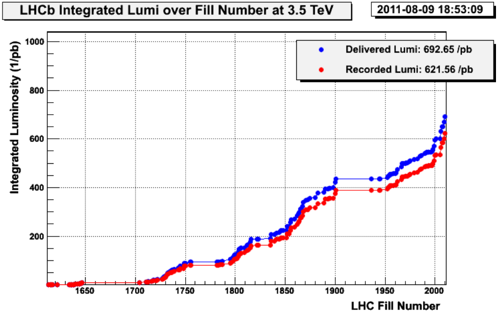

# Outline

$$B_{s,d} \to \mu^+\mu^-$$

See talk by Marc-Olivier Bettler on Friday

$$B_d \to K^{*0}\mu^+\mu^-$$
$$(b \to s\ell^+\ell^-)$$

With $309\,\mathrm{pb}^{-1}$ of integrated luminosity collected by LHC*b* in 2011

# The rare decay $B_d \to K^{*0}\mu^+\mu^-$

- $B_d \to K^{*0}\mu^+\mu^-$ is a FCNC process mediated by electroweak penguin and box diagrams in the SM
- Sensitive to new physics with contributions from:
  - right-handed currents.
  - new scalar / pseudo-scalar operators.

  by probing helicity structure of the decay through angular observables.

- Decay described by three angles ($\theta_L$, $\theta_K$ and $\phi$) and the dimuon invariant mass squared, $q^2$.
- Many observables where leading form-factor uncertainties can be cancelled, e.g forward-backward asymmetry of the muons ($A_{FB}$).

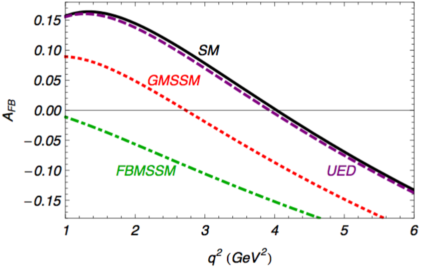


W.Altmannshofer et al. [JHEP 0901:019 (2009)]

# $B_d \to K^{*0}\mu^+\mu^-$ event selection

- Events are triggered on:
  - L0: A single high-$p_T$ muon
  - HLT 1: A single high-IP and high-$p_T$ track.
  - HLT 2: The topology of the $B_d$ decay.
- Boosted Decision Tree used offline to reduce combinatorial background. Trained on $B_d \to K^{*0} J/\psi$ and background candidates from the upper mass sideband in the 2010 data.
- Cleanly select $302 \pm 20$ $B_d \to K^{*0}\mu^+\mu^-$ candidates with background-to-signal of $\sim 0.3$.

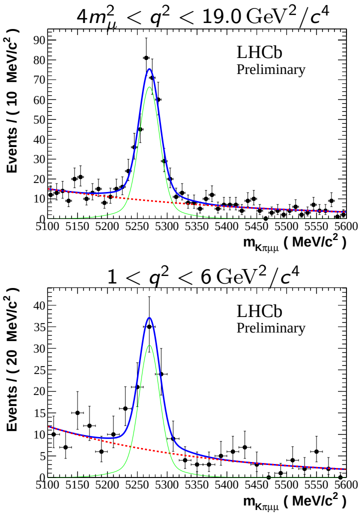

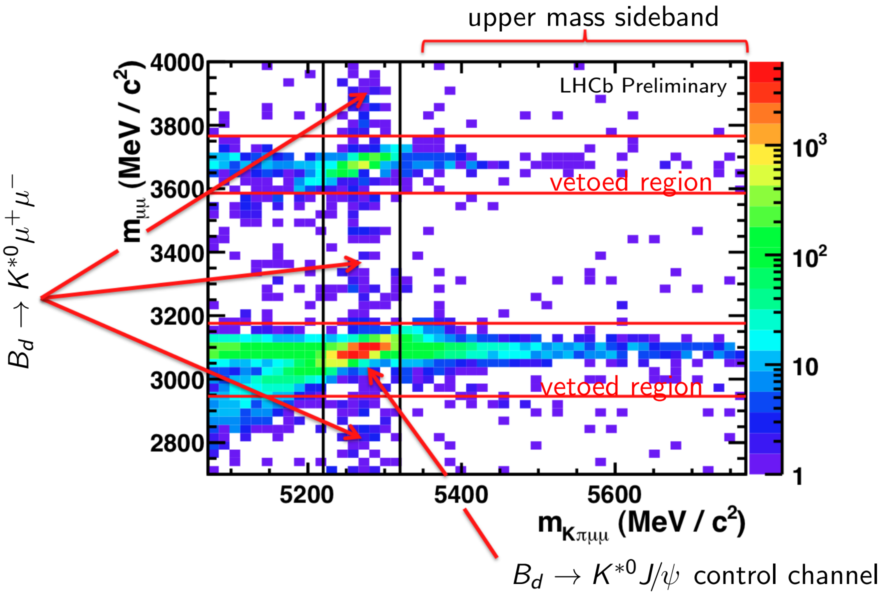
upper mass sideband
LHCb Preliminary
vetoed region
vetoed region
$B_d \to K^{*0}\mu^+\mu^-$
$m_{\mu\mu}$ (MeV / c$^2$)
4000
3800
3600
3400
3200
3000
2800
5200
5400
5600
$m_{K\pi\mu\mu}$ (MeV / c$^2$)
$10^3$
$10^2$
10
1
$B_d \to K^{*0} J/\psi$ control channel

# $B_d \to K^{*0}\mu^+\mu^-$ exclusive backgrounds

- Specific peaking backgrounds rejected by PID cuts and cuts on wrong mass hypothesis. e.g.:

  $B_d \to K^{*0}(\to K\pi\{\to \mu\})J/\psi(\to \mu\mu\{\to \pi\})$

  $B_s \to \phi(\to KK\{\to \pi\})\mu^+\mu^-$

- ‘Peaking’ backgrounds reduced to $< 3\%$ of signal.
- $K^{*0} \to \overline{K}^{*0}$ mis-id, which would dilute $A_{FB}$, is reduced to 0.7%.

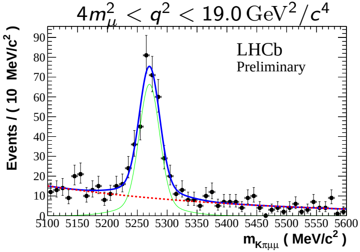


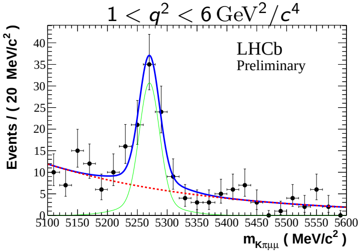

# $B_d \to K^{*0}\mu^+\mu^-$ event yields in $q^2$ bins

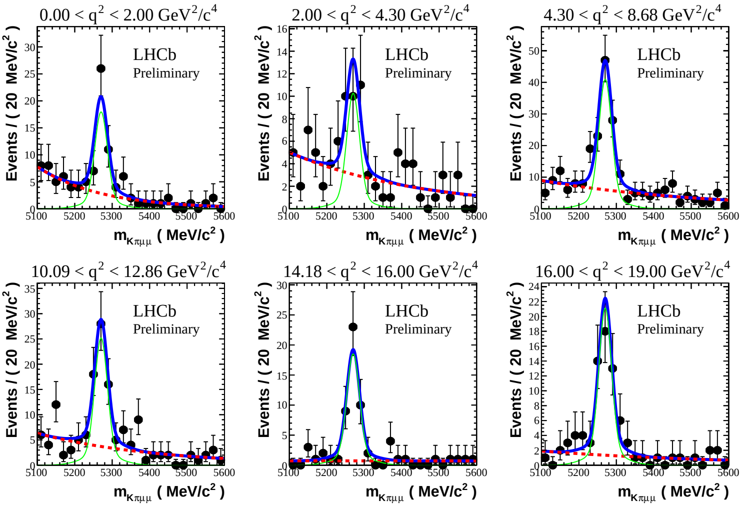

# $B_d \to K^{*0}\mu^+\mu^-$ acceptance correction

- Detector geometry, track reconstruction, the trigger and offline selection introduce a $\theta_L$, $\theta_K$ and $q^2$ dependent acceptance bias.

- Acceptance dominated by detector 'geometry' and reconstruction (e.g. $p > 3\,\mathrm{GeV}/c$ for muon to reach muon stations). Trigger and selection optimised to reduce additonal biases.
- Candidates are efficiency corrected event-by-event using MC that has been validated and corrected for data-MC differences in:
  - Tracking efficiency.
  - Hadron (mis-)identification.
  - Muon (mis-)identification.
  - Impact parameter resolution
  - $B_d$ kinematics . . .

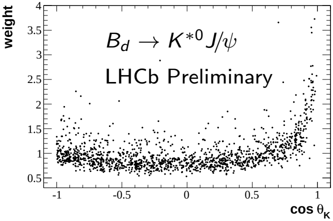


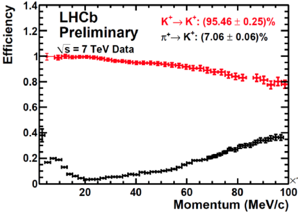

# Differential branching fraction

- Applying efficiency correction and normalising w.r.t $B_d \to K^{*0} J/\psi$:

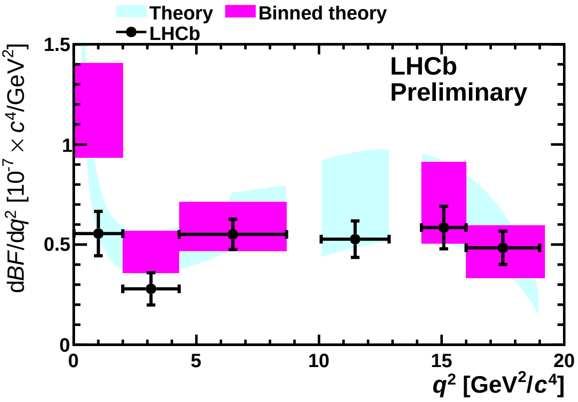


Theory prediction from C. Bobeth et al. [arXiv:1105.0376v2]

# Differential branching fraction

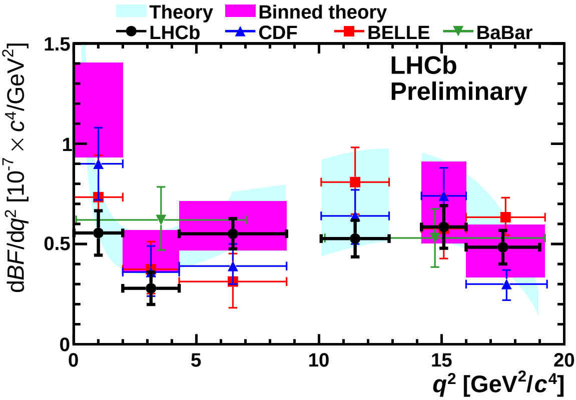


BaBar [PRD **79** (2009)], Belle [PRL **103** (2009)], CDF [PRL **106** (2011)]

# Extracting angular observables

- Perform an unbinned maximum likelihood fit in $q^2$-bins, weighting events event-by-event.
- Simultaneously fit $m_{K\pi\mu\mu}$, $\cos\theta_K$ and $\cos\theta_\ell$ with:

$$\frac{1}{\Gamma}\frac{\mathrm{d}^2\Gamma}{\mathrm{d}\cos\theta_\ell\,\mathrm{d}q^2} = \frac{3}{4}F_L(1-\cos^2\theta_\ell) + \frac{3}{8}(1-F_L)(1+\cos^2\theta_\ell) + A_{FB}\cos\theta_\ell$$

$$\frac{1}{\Gamma}\frac{\mathrm{d}^2\Gamma}{\mathrm{d}\cos\theta_K\,\mathrm{d}q^2} = \frac{3}{2}F_L\cos^2\theta_K + \frac{3}{4}(1-F_L)(1-\cos^2\theta_K)$$

.

for the signal angular distributions, a double Gaussian distribution for the signal mass distribution

- An exponential for the background mass distribution and $2^{nd}$ order polynomials for the angular distributions of the background.

# Validation with $B_d \to K^{*0} J/\psi$

- Validate the fit using $B_d \to K^{*0} J/\psi(\to \mu^+\mu^-)$ decays.
- $A_{FB}$ is consistent with zero. $F_L$ is consistent with measurements from *BABAR*, Belle and 2010 LHCb result.
  - $S$-wave dependence in $\cos\theta_K$ consistent with observations of *BABAR* [PRD **76** (2007)].
- Contributions from non $K^{*0}(892) \to K\pi$, such as non-resonant $K\pi$ or $K\pi$ S-wave are ignored for the $B_d \to K^{*0}\mu^+\mu^-$ analysis†.

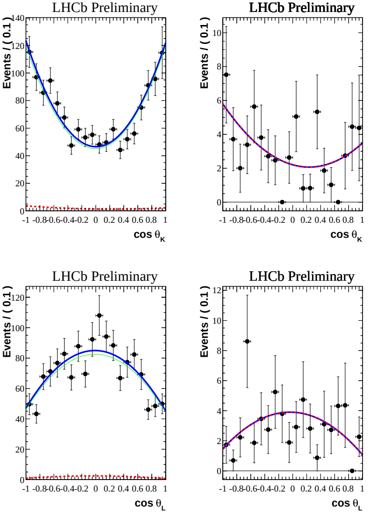


† theory input is needed here

# Forward-backward asymmetry

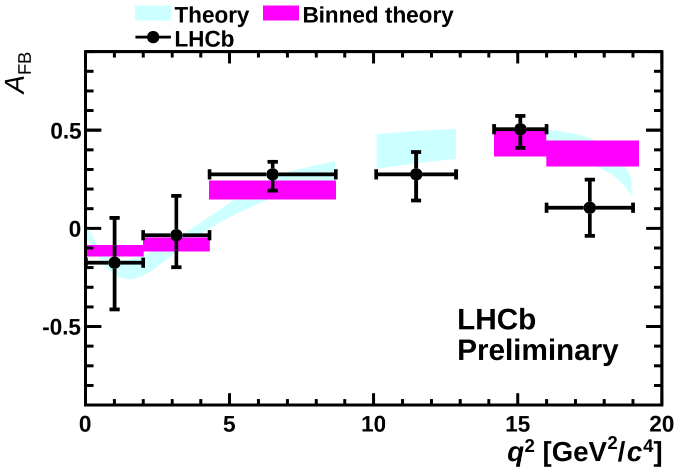


Theory prediction from C. Bobeth et al. [arXiv:1105.0376v2]

# Forward-backward asymmetry

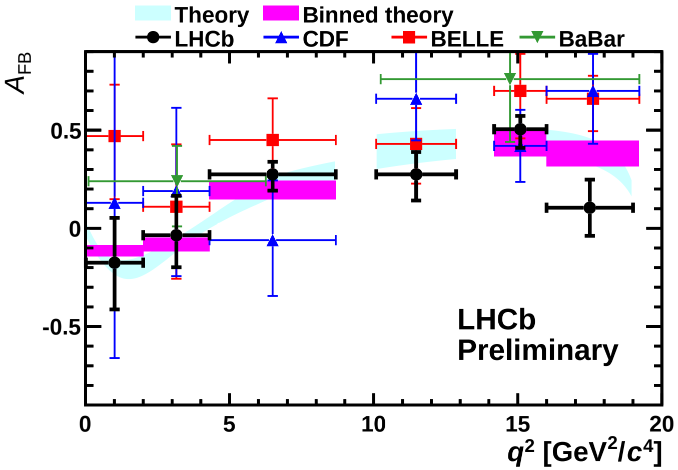


BaBar [PRD **79** (2009)], Belle [PRL **103** (2009)], CDF [PRL **106** (2011)]

# Longitudinal polarisation

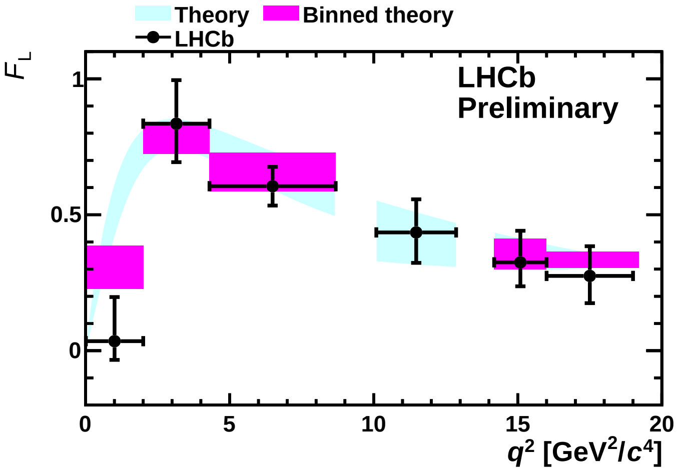


Theory prediction from C. Bobeth et al. [arXiv:1105.0376v2]

# Longitudinal polarisation

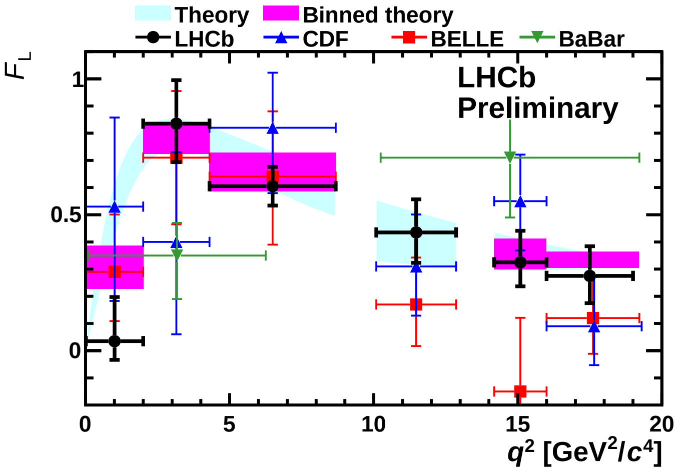


BaBar [PRD **79** (2009)], Belle [PRL **103** (2009)], CDF [PRL **106** (2011)]

# $B_d \to K^{*0}\mu^+\mu^-$ systematic uncertainties

- Consider sources of systematic uncertainty from:
  1. Data derived MC corrections, which are varied systematically within their measured uncertainties:
     - Variation of PID performance, impact parameter resolution, track reconstruction efficiency and trigger $p_T$ dependence.
  2. MC statistics (dominant at high-$q^2$ in the phase space MC).
  3. Signal and background mass models.
  
  (4.) Background angular model for $A_{FB}$ and $F_L$.
  
  (5.) The uncertainty on the $B_d \to K^{*0} J/\psi$ BF for BF normalisation.
- Systematic uncertainty is typically $\mathcal{O}(30\%)$ of statistical uncertainty. Sources of systematic uncertainty are statistically limitted and expected to improve with larger data sets.

# $B_d \to K^{*0}\mu^+\mu^-$ summary

- This preliminary result, based on $309\mathrm{pb}^{-1}$, represents the most precise measurement of $B_d \to K^{*0}\mu^+\mu^-$ to date.
- $\mathrm{d}BF/\mathrm{d}q^2$, $A_{FB}$ and $F_L$ show a striking agreement with recent SM predictions, with:

$$\begin{aligned} A_{FB} &= -0.10^{+0.14}_{-0.14} \pm 0.05 \\ F_L &= 0.57^{+0.11}_{-0.10} \pm 0.03 \\ \mathrm{d}BF/\mathrm{d}q^2 &= 0.39 \pm 0.06 \pm 0.02 \end{aligned}$$

  in the theoretically favoured $1 < q^2 < 6\,\mathrm{GeV}^2/c^4$ region.
- The measurement is statistically dominated and the leading systematic uncertainties are also expected to improve with increased statistics.

$$B_d \to K^{*0}\gamma \;\&\; B_s \to \phi\gamma$$
$$(b \to s\gamma)$$

With $88\,\mathrm{pb}^{-1}$ of integrated luminosity collected in 2010 and 2011

# $B_d \to K^{*0}\gamma$ & $B_s \to \phi\gamma$

- BR($B_d \to X_s\gamma$) in agreement with SM predictions:

$$BR(B_d \to X_s\gamma)_{\rm exp.} = 3.15 \pm 0.23 \times 10^{-4}$$ [PRL **103** (2009)]

$$BR(B_d \to X_s\gamma)_{\rm th.} = 3.56 \pm 0.26 \times 10^{-4}$$ M. Misiak [PRL **98** (2007)]

  setting strong constraints on NP.

- Large deviations still possible in asymmetries, e.g. $\mathcal{A}_{CP}(B_d \to K^{*0}\gamma)$. Worlds best measurement of $\mathcal{A}_{CP}(B_d \to K^{*0}\gamma)$ from *BABAR* based on 2400 signal candidates:

$$\mathcal{A}_{CP} = -0.016 \pm 0.022 \pm 0.007$$ [PRL **103** (2009)]

- Can also probe the right-handed component of the photon polarisation (and $\mathcal{C}_7'$) through the time dependent CP asymmetry of $B_s \to \phi\gamma$ (or through an angular analysis of $B_d \to K^* e^+ e^-$ at low-$q^2$ [LHCb-PUB-2009-008]).

# $B_d \to K^{*0}\gamma$ & $B_s \to \phi\gamma$ at LHCb

- Common selection for $B_d \to K^{*0}\gamma$ and $B_s \to \phi\gamma$. Differs only in daughter PID requirements and $K^{*0}/\phi$ mass window.
- Observe:
  - $485 \pm 43$ $B_d \to K^{*0}\gamma$
  - $60 \pm 12$ $B_s \to \phi\gamma$

  candidates in $88\,\mathrm{pb}^{-1}$.
- Aim to measure $\mathcal{B}(B_s \to \phi\gamma)$ to $\mathcal{O}(20\%)$ precision by end of summer. c.f. $\mathcal{O}(35\%)$ by Belle [PRL **100** (2008)].
- Aim for measurement of $\mathcal{A}_{CP}(B_d \to K^{*0}\gamma)$ for winter conferences.

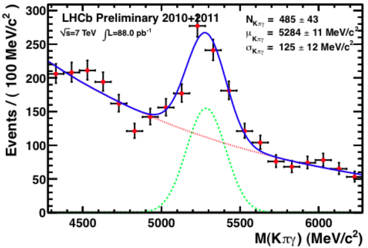


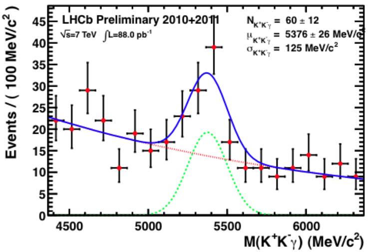

## Summary

LHC and LHCb performance in 2011 has been excellent.

$620\,\text{pb}^{-1}$ integrated luminosity collected in 3 months in 2011. Expect $1\,\text{fb}^{-1}$ by the end of the year.

First measurement of angular observables in $B_d \to K^{*0}\mu^+\mu^-$ by LHC$b$ appears consistent with the SM.

## Expect numerous rare decay results in 2011-2012

- Large number of ongoing analysis:

$R_K$ | $D^0 \to \mu^+\mu^-$ | $B_s \to \phi\mu^+\mu^-$ | $\Lambda_B \to \Lambda\mu^+\mu^-$

$B^+/D^+_{(S)} \to K^-\mu^+\mu^+$ | $D \to K^+K^-\mu^+\mu^-$ | $B_d \to K^{*0}e^+e^-$

$B \to e\mu(\mu\tau)$ | $\tau^+ \to \mu^+\mu^-\mu^+$ | $B_s \to \phi\gamma$ | $B_d \to K^{*0}\gamma$

$B_d \to K^{*0}\mu^+\mu^-$ | $B_{s,d} \to \mu^+\mu^-$ | Isospin analysis in $B_{u,d} \to X_{s(u,d)}\mu^+\mu^-$

$$B^+ \to h^- \mu^+ \mu^+$$

(not an electroweak penguin)

With $36\,\mathrm{pb}^{-1}$ of integrated luminosity collected by LHC*b* in 2010

# Lepton number violation through $B^+ \to h^-\mu^+\mu^+$ decays

- Search for number violation in $B^+ \to K^-\mu^+\mu^+$ and $B^+ \to \pi^-\mu^+\mu^+$ decays. These are $\Delta$L=2 processes that are forbidden in SM (unambiguous sign of NP).
- Decay can be mediated by a heavy $\mathcal{O}(1\,\mathrm{GeV}/c^2)$ Majorana neutrino (that mixes with SM $\nu_\mu$).

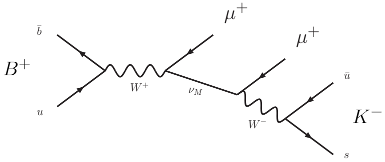


- Existing limits from [CLEO] are $1-2\times 10^{-6}$.

# Lepton number violation through $B^+ \to h^- \mu^+ \mu^+$ decays

- Analysis strategy:
  - Normalise branching fraction to $B^+ \to K^+ J/\psi$ in data.
  - Peaking backgrounds estimated to be negligible using MC (to model the kinematics) and data derived particle mis-id rates.
- Observe **no** candidates and set limits of:

$$\mathcal{B}(B^+ \to K^- \mu^+ \mu^+) < 4.1 \times 10^{-8}$$

$$\mathcal{B}(B^+ \to \pi^- \mu^+ \mu^+) < 4.4 \times 10^{-8}$$

at 90% CL.

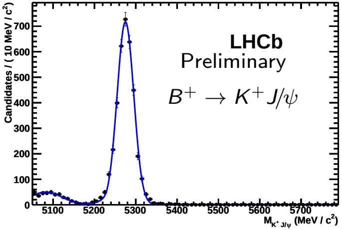


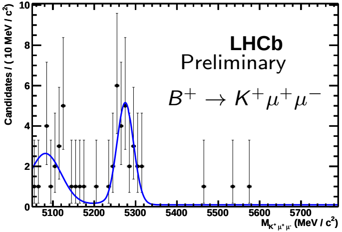

# $B^+ \to h^-\mu^+\mu^+$ exclusive peaking backgrounds

- The expected exclusive peaking backgrounds in $36\,\mathrm{pb}^{-1}$ after applying the kinematic selection and parametrically applying the detector PID performance:

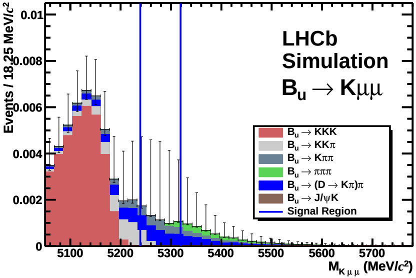


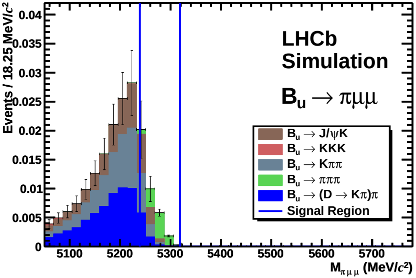


- All exclusive background contributions are well below 0.1 event for $B^+ \to K^-\mu^+\mu^+$ and $B^+ \to \pi^-\mu^+\mu^+$.

$$B_d \to K^{*0}\mu^+\mu^-$$
$$(b \to s\ell^+\ell^-)$$

With $309\,\mathrm{pb}^{-1}$ of integrated luminosity collected by LHC*b* in 2011

# $B_d \to K^{*0}\mu^+\mu^-$ likelihoods

- Profiled $-\log\mathcal{L}$ in the physically allowed region of $A_{FB}$ and $F_L$.

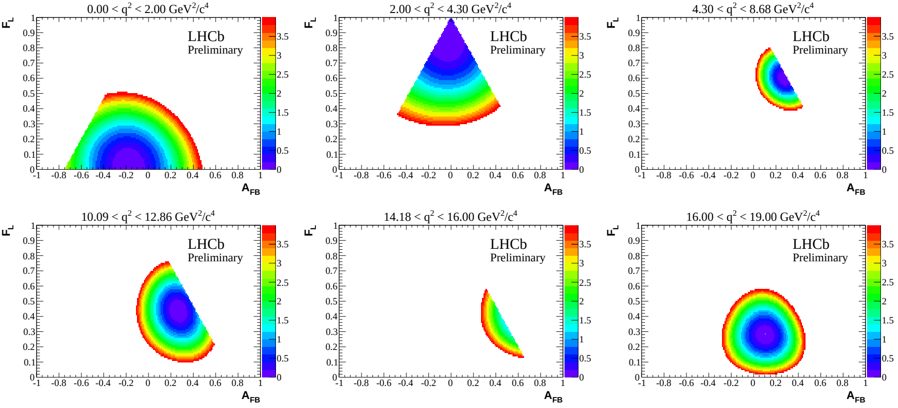

# $B_d \to K^{*0}\mu^+\mu^-$ event yields

- Observed (raw) $B_d \to K^{*0}\mu^+\mu^-$ signal and background yields in a $5220 < m_{K\pi\mu\mu} < 5320\,\mathrm{MeV}/c^2$ mass window in 309 $\mathrm{pb}^{-1}$ using the $q^2$ binning from Belle.

| $q^2(\mathrm{GeV}^2)$ | $n_{sig}$ | $n_{bkg}$ | significance ($\sigma$) |
|---|---|---|---|
| $0 < q^2 < 2$ | $40.9 \pm 7.5$ | $14.4 \pm 8.5$ | 7.7 |
| $2 < q^2 < 4.3$ | $23.3 \pm 6.2$ | $15.3 \pm 8.6$ | 4.9 |
| $4.3 < q^2 < 8.68$ | $93.3 \pm 11.3$ | $30.0 \pm 12.5$ | 11.7 |
| $10.09 < q^2 < 12.9$ | $57.3 \pm 8.8$ | $18.6 \pm 9.7$ | 9.3 |
| $14.18 < q^2 < 16$ | $42.2 \pm 6.8$ | $3.6 \pm 4.7$ | 10.1 |
| $16 < q^2 < 19$ | $48.1 \pm 7.8$ | $6.7 \pm 6.4$ | 9.2 |
| $1 < q^2 < 6\,\mathrm{GeV}^2$ | $70.0 \pm 10.2$ | $32. \pm 3.2$ | 9.4 |
| Full | $302.3 \pm 20.1$ | $91.0 \pm 5.4$ | – |

- In the full mass window $323.0 \pm 21.4$ $B_d \to K^{*0}\mu^+\mu^-$ candidates are observed.

# $B_d \to K^{*0}\mu^+\mu^-$ fit results in $q^2$ bins

- The central values and statistical and systematic uncertanties for $A_{FB}$, $F_L$ and $\mathrm{dB}Factory/\mathrm{d}q^2$ in the six $q^2$ bins and the $1 < q^2 < 6\,\mathrm{GeV}^2$ bin.

| $q^2(\,\mathrm{GeV}^2)$ | $A_{FB}$ | $F_L$ | $\mathrm{d}\,BF/\mathrm{d}q^2$ $(\times 10^{-7})$ |
|---|---|---|---|
| $0 < q^2 < 2$ | $-0.17^{+0.22}_{-0.23} \pm 0.06$ | $0.03^{+0.15}_{-0.03} \pm 0.06$ | $0.56 \pm 0.11 \pm 0.03$ |
| $2 < q^2 < 4.3$ | $-0.04^{+0.19}_{-0.15} \pm 0.06$ | $0.84^{+0.15}_{-0.13} \pm 0.06$ | $0.28 \pm 0.08 \pm 0.02$ |
| $4.3 < q^2 < 8.68$ | $0.28^{+0.06}_{-0.08} \pm 0.02$ | $0.60^{+0.07}_{-0.07} \pm 0.01$ | $0.55 \pm 0.07 \pm 0.03$ |
| $10.09 < q^2 < 12.9$ | $0.27^{+0.11}_{-0.13} \pm 0.03$ | $0.44^{+0.12}_{-0.11} \pm 0.02$ | $0.53 \pm 0.09 \pm 0.03$ |
| $14.18 < q^2 < 16$ | $0.50^{+0.06}_{-0.09} \pm 0.03$ | $0.33^{+0.11}_{-0.08} \pm 0.04$ | $0.59 \pm 0.10 \pm 0.03$ |
| $16 < q^2 < 19$ | $0.10^{-0.13}_{-0.13} \pm 0.06$ | $0.28^{+0.10}_{-0.09} \pm 0.04$ | $0.48 \pm 0.08 \pm 0.03$ |
| $1 < q^2 < 6$ | $-0.10^{+0.14}_{-0.14} \pm 0.05$ | $0.57^{+0.11}_{-0.10} \pm 0.03$ | $0.39 \pm 0.06 \pm 0.02$ |

- The first, asymmetric, set of errors is given by a Bayesian error estimate, with a prior that the points sit within the physical region. The second error is a systematic error

# The Effective Hamiltonian

- Model independent approach. Are there new heavy degrees of freedom $\rightarrow$ NP ?
- Form effective Hamiltonian for $b \rightarrow s$ transitions :

$$\mathcal{H}_{eff} = \frac{4G_F}{\sqrt{2}} V_{tb} V_{ts}^{*} \sum_i \left[ \mathcal{C}_i \mathcal{O}_i + \mathcal{C}_i^{\prime} \mathcal{O}_i^{\prime} \right]$$

Short range physics (heavy degrees of freedom) are contained in the coefficients, $\mathcal{C}_i$, and the operators $\mathcal{O}_i$ contain the long range contributions.

# Operator product expansion for $b \to s\ell\ell$

- Three distinct energy scales:
  - $\mathcal{O}(\Lambda_{\rm QCD}) \sim 0.1\,\mathrm{GeV}$, $\mathcal{O}(m_b) \sim 5\,\mathrm{GeV}$ and $\mathcal{O}(m_W) \sim 90\,\mathrm{GeV}$.
- Factor out long and short distance components:

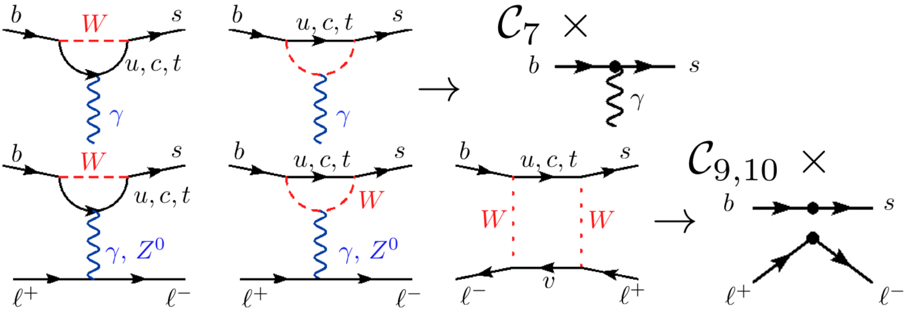

# $B_d \to K^{*0}\mu^+\mu^-$ as a probe of New Physics

- Sensitive to NP with contributions from:
  - right-handed currents.
  - new scalar, pseudo-scalar or tensor operators.

  predominantly through angular observables (probing helicity structure of the underlying theory).

| $\leftarrow 1\text{fb}^{-1}$ | $1\text{–}\ 2\text{fb}^{-1}$ | $2 \to 10\text{fb}^{-1}$ ( $\int \mathcal{L}dt$ at LHCb ) |
|---|---|---|
| $A_{FB}(q^2)$ | $A_T^{(2)}$ | **Full angular analysis of Helicity/Transveristy amplitudes** |
| $\frac{d\Gamma}{dq^2}$ | | CP asymmetries in angular observables |
| $F_L$ | | Isospin analysis |

- Calculable away from the $c\bar{c}$ resonances and for $m_{\mu^+\mu^-} > 1\,\text{GeV}$.

# Angular basis for $B_d \to K^{*0}\mu^+\mu^-$

- $q^2$ Invariant mass squared of the dimuon system $q^2 = m^2_{\mu^+\mu^-}$.
- $\theta_\ell$ Angle between the direction of the $\mu^-$ in the $\mu^+\mu^-$ rest frame and the direction of the $\mu^+\mu^-$ in the $\overline{B}_d$ rest frame.
- $\theta_K$ Angle between the kaon in the $\overline{K}^{*0}$ rest frame and the $\overline{K}^{*0}$ in the $\overline{B}_d$ rest frame.
- $\phi$ Angle between planes defined by $\mu^-$ $\mu^+$ and the $K\pi$ in the $\overline{B}_d$ frame.

$\overline{B}_d \to \overline{K}^{*0}\ell^+\ell^-$ angular definition

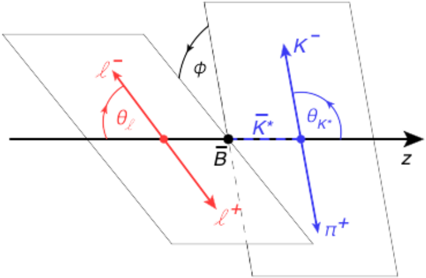

# Angular distribution for $B_d \to K^{*0}\mu^+\mu^-$

- The full angular distribution can be written in term of 6 complex, $q^2$-dependent, helicity or transveristy amplitudes. e.g. $A_{0,\mathrm{L/R}}$, $A_{\parallel,\mathrm{L/R}}$ and $A_{\perp,\mathrm{L/R}}$.

or equivalently as 12 $q^2$-dependent angular terms:

$$\frac{\mathrm{d}^4\Gamma}{\mathrm{d}\cos\theta_\ell\,\mathrm{d}\cos\theta_K\,\mathrm{d}\phi\,\mathrm{d}q^2} = \frac{9}{32\pi}\cdot\Big[\, I_1^S \sin^2\theta_K + I_1^C \cos^2\theta_K + (I_2^S \sin^2\theta_K + I_2^C \cos^2\theta_K)\cos 2\theta_\ell$$
$$I_3 \sin^2\theta_K \sin^2\theta_\ell \cos 2\phi + I_4 \sin 2\theta_K \sin 2\theta_\ell \cos\phi$$
$$I_5 \sin 2\theta_K \sin\theta_\ell \cos\phi + (I_6^S \sin^2\theta_K + I_6^C \cos^2\theta_K)\cos\theta_\ell$$
$$I_7 \sin 2\theta_K \sin\theta_\ell \sin\phi + I_8 \sin 2\theta_K \sin 2\theta_\ell \sin\phi$$
$$I_9 \sin^2\theta_K \sin^2\theta_\ell \sin 2\phi \;\Big]$$

# Angular projections for $B_d \to K^{*0}\mu^+\mu^-$

- Integrating over all but one of the angles yields:

$$\frac{1}{\Gamma}\frac{\mathrm{d}^2\Gamma}{\mathrm{d}\cos\theta_\ell\,\mathrm{d}q^2} = \frac{3}{4}F_L(1-\cos^2\theta_\ell) + \frac{3}{8}(1-F_L)(1+\cos^2\theta_\ell) + A_{FB}\cos\theta_\ell$$

$$\frac{1}{\Gamma}\frac{\mathrm{d}^2\Gamma}{\mathrm{d}\cos\theta_K\,\mathrm{d}q^2} = \frac{3}{2}F_L\cos^2\theta_K + \frac{3}{4}(1-F_L)(1-\cos^2\theta_K)$$

$$\frac{1}{\Gamma}\frac{\mathrm{d}^2\Gamma}{\mathrm{d}\phi\,\mathrm{d}q^2} = 1 + \frac{1}{2}A_T^2(1-F_L)\cos 2\phi + A_{\mathrm{Im}}\sin 2\phi$$

where :

$$A_{FB} = \frac{3}{2}\frac{\mathcal{R}e(A_{\parallel,\mathrm{L}}A^*_{\perp,\mathrm{L}}) - \mathcal{R}e(A_{\parallel,\mathrm{R}}A^*_{\perp,\mathrm{R}})}{|A_0|^2+|A_\parallel|^2+|A_\perp|^2} \quad \text{and} \quad F_L = \frac{|A_0|^2}{|A_0|^2+|A_\parallel|^2+|A_\perp|^2}$$

# Forward backward asymmetry

- With small data-sets focus on $A_{FB}$, the forward-backward asymmetry of the muons. Highly sensitive to NP contributions.
- Hadronic uncertainties from Form Factors ($V$, $T_{1,2}$ & $A_1$) cancel at LO when $A_{FB} = 0$.

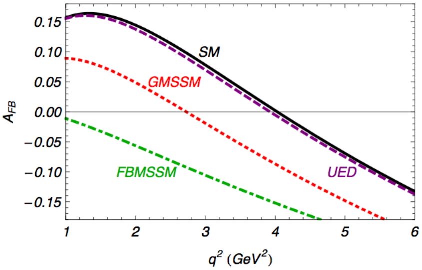


[W.Altmannshofer et al.]

$$A_{FB}(q^2) = \frac{N(\cos\theta_\ell > 0) - N(\cos\theta_\ell < 0)}{N(\cos\theta_\ell > 0) + N(\cos\theta_\ell < 0)}$$
$$= \frac{1}{\Gamma}\frac{3}{4}(I_6^s + I_6^c)$$
$$\propto f(\hat{s})|V_{ts}^* V_{tb}|\mathcal{C}_{10}\left(\mathcal{R}e(C_9^{(eff)})VA_1 + \frac{\hat{m}_b}{\hat{s}}\mathcal{C}_7^{(eff)}\left[VT_2(1-\hat{m}_{K^*}) + A_1T_1(1+\hat{m}_{K^*})\right]\right)$$

# Constructing asymmetries from transversity amplitudes

- With a large data set can explore new angular observables through a full angular analysis. Construct observables independent of form factors (at LO in $\Lambda/m_b$ and $\alpha_s$). e.g. $A_T^{(3)}$ sensitive to new physics in $\mathcal{C}_7'$.

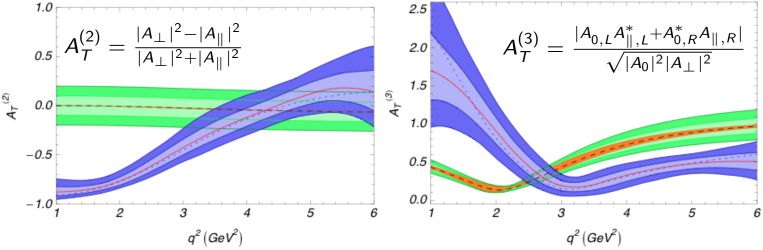


blue band: Experimental error on a SUSY scenario with a large gluino mass from 10 fb$^{-1}$ toy experiments.

green band: Standard model prediction with theory error. [U. Egede et al.]

# The LHCb trigger

- L0 Hardware trigger, reduces rate from 40 MHz to 1 MHz by triggering on high-$p_T$ lepton or hadron.
- HLT 1 Software trigger in event filter farm. Reduces rate to 35 kHz by reconstructing tracks with high-IP and $p_T$/ finding displaced verticies in VELO.
- HLT 2 Software trigger reduces rate to tape to 2 kHz. Performs global reconstruction and inclusively/exclusively selects $B$ or $D$ mesons.

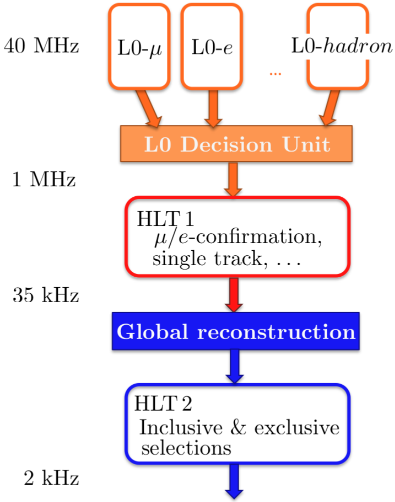

## Acceptance effects in the LHCb reconstruction

- Plots show impact of the muon reconstruction on $\theta_\ell$ at low-$q^2$ and impact of the pion and kaon reconstruction on $\theta_K$ at intermediate-$q^2$.
- Soft pion $\rightarrow$ asymmetric acceptance in $\theta_K$.
- Efficiency lowest at $q^2 \rightarrow (m_B - m_{K^{*0}})^2$ where the $K^{*0}$ is softest.

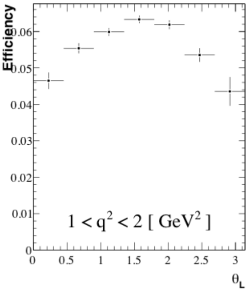


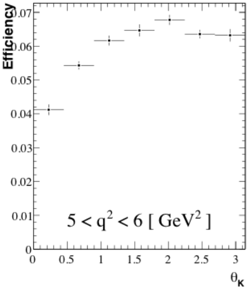

$$B_d \to K^{*0}\gamma \ \& \ B_s \to \phi\gamma$$
$$(b \to s\gamma)$$

With $88\,\mathrm{pb}^{-1}$ of integrated luminosity collected in 2010 + 2011

# $B_d \to K^{*0}\gamma$ & $B_s \to \phi\gamma$ trigger strategy

- Trigger strategy for radiative decays:
  - L0 Trigger on high-$E_T$ photon.
  - HLT 1 Trigger on high-$p_T$ and high-IP track or on softer track and high-$E_T$ photon.
  - HLT 2 Full exclusive reconstruction of the $K^{*0}\gamma$ or $\phi\gamma$ candidate.